DEVELOPMENT OF IMPROVED SINGLE CRYSTAL GALLIUM PHOSPHIDE SOLAR CELLS

Quarterly Report No. 1

12 June - 12 September 1963

52p.

(NASA Contract No., NAS3-2776)

Placed by (NASA CR-52140)

W. O. Groves and A. S. Epstein [1963] 52p refr

NATIONAL AERONAUTICS AND SPACE ADMINISTRATION

Lewis Research Center

Cleveland, Ohio

MONSANTO RESEARCH CORPORATION

A SUBSIDIARY OF MONSANTO CHEMICAL COMPANY

DAYTON LABORATORY

DAYTON 7, OHIO

Requests for copies of this report should be referred to:

National Aeronautics and Space Administration
Office of Scientific and Technical Information
Washington, D. C., 20546
Attn: AFSS-A

NOTICE

This report was prepared as an account of Government-sponsored work. Neither the United States nor the National Aeronautics and Space Administration (NASA), nor any person acting on behalf of NASA:

A) Makes any warranty or representation expressed or implied with respect to the accuracy, completeness, or usefulness of the information contained in this report or that the use of any information apparatus, method, or process disclosed in this report may not infringe privately-owned rights; or

B) Assumes any liabilities with respect to the use of, or for damages resulting from the use of any information apparatus method or process disclosed in this report.

As used above, "person acting on behalf of NASA" includes any employee or contractor of NASA or employee of such contractor, to the extent that such employee or contractor of NASA, or employee of such contractor prepares, disseminates, or provides access to, any information pursuant to his employment or contract with NASA, or his employment with such contractor.

DEVELOPMENT OF IMPROVED SINGLE CRYSTAL GALLIUM PHOSPHIDE SOLAR CELLS

Quarterly Report No. 1
June 12, 1963 to September 12, 1963

Contract No. NAS3-2776

NATIONAL AERONAUTICS AND SPACE ADMINISTRATION

Technical Management
Space Power Systems Division
NASA - Lewis Research Center
Attention: Clifford K. Swartz

Report Prepared by: W. O. Groves and A. S. Epstein
Edited by: R. A. Ruehrwein

Work Performed by:

Central Research Department
MONSANTO CHEMICAL COMPANY
St. Louis, Missouri

TABLE OF CONTENTS

		Page Number
I.	PURPOSE	1.
II.	ABSTRACT	2.
III.	MATERIAL PREPARATION	3.
	A. Epitaxial Deposition	3.
	B. Electrical Properties	7.
IV.	SOLAR CELL FABRICATION	8.
	A. Diffusion	8.
	B. Junction Delineation	10.
	C. Contacts	10.
	D. Etching	11.
V.	EVALUATION	11.
	A. Solar Cell Characteristics	11.
	B. Sheet Resistance and Surface Concentration	13.
	C. Spectral Response	14.
	D. Effects of GaP-GaAs Interface	15.
	E. Junction Characteristics	16.
VI.	CONCLUSIONS	18.
VII.	FUTURE STUDIES	18.
VIII.	REFERENCES	20.

I. PURPOSE

This report presents the work done during the first quarter of the Single Crystal Gallium Phosphide Solar Cell program. The objective of this program is the development of an efficient solar cell operable at temperatures up to 500° C. The approach is to grow single crystal gallium phosphide by epitaxial deposition from the vapor phase on gallium arsenide substrate followed by removal of the gallium arsenide. Diffused junction cells are then fabricated and the photovoltaic properties of the cells are measured, ultimately up to 500° C. The design and performance of the cells are to be related to the electrical and optical properties of the gallium phosphide.

II. ABSTRACT

/0///

Single crystal gallium phosphide was prepared by epitaxial deposition on single crystal gallium arsenide using hydrogen chloride in an open tube vapor transport process with either gallium phosphide or gallium plus phosphorus sources. Good epitaxial interfaces were achieved by pretreating the substrate with hydrogen and phosphorus at high temperatures.

Zinc diffusion profiles in the gallium phosphide were not planar because of structural imperfections in the material and the P-N junctions exhibited large leakage. In measurements of solar cell characteristics photocells gave open circuit voltages up to 0.8 volt and short circuit currents up to 0.2 ma/cm^2. The low collection efficiency may be attributed to short minority carrier lifetime.

AUTHOR

III. MATERIAL PREPARATION

A. Epitaxial Deposition

An open tube transport process for epitaxial growth using a dilute mixture of hydrogen chloride in hydrogen as the carrier gas has been described previously[1]. This process has been used in the present work, with source temperature of 890° to 980° C and deposition temperatures of 800° to 850° C, to grow monocrystalline gallium phosphide layers on < 100 > oriented gallium arsenide substrates. In some experiments gallium was used as the source in place of gallium phosphide, elemental phosphorus being vaporized into the gas stream from a third temperature zone in the reactor. A schematic of the system is shown in Figure 1.

Initial objectives have been to prepare epitaxial GaP layers suitable for testing of solar cell fabrication techniques. Surfaces of GaP previously grown on GaAs had generally been of poor quality, the defects - broad bumps, holes, and others tentatively identified as stacking faults - were believed to cause the non-planar P-N junctions formed on diffusion. In addition GaP-GaAs interfaces had been irregular, in extreme cases containing large voids. All of these defects may have been due directly or indirectly to surface contamination of the substrate. Efforts have been directed toward eliminating these defects and to growing thick layers of GaP from which the substrate might be removed.

In two initial experiments an attempt was made to eliminate the interface irregularity by growing a graded GaAs-GaP interlayer before depositing 100% GaP, a technique employing separate GaAs and GaP sources, previously found successful. Although interlayers about five microns thick and graded from about 40 to 100 mole % GaP were obtained, the interface irregularity was not completely eliminated and the surfaces of the 35 micron thick layers were again rather poor. Surface contamination may have been a problem. Subsequently, as will be described later, it was found possible to obtain a very nearly smooth planar interface without resorting to a graded interlayer and therefore these efforts were discontinued.

To determine the effect of starting conditions on the substrate surface, using a source of gallium and elemental phosphorus, a run was discontinued after maintaining phosphorus vapor flow for twenty minutes with the system at temperature. Hydrogen chloride was not introduced. This treatment produced a microscopically

rough mat surface on which a number of small nodular growths were evident (presumably via oxygen transport). Subsequent deposition of a thin layer of GaP produced surfaces containing bumps in roughly the same frequency as the nodular growths. While it thus seems probable that the bumps had been nucleated during the start up period, whether this was due to a surface condition of the substrate or contamination in the gas stream, or both, is not clear.

Following the experiment just described an attempt was made to clean the surfaces for further deposition by heating the wafers to 1000° C in phosphorus vapor carried by hydrogen. This produced a light etching of the GaP as evidenced by a slight change in texture and a rounding of bump edges. The treatment was then repeated, followed immediately by reduction of source and substrate temperatures and introduction of HCl. The surface of the GaP layer formed on a fresh GaAs substrate monitor Hall bar included in this final step was virtually free of defects of the type referred to above. However, the other wafers, previously deposited, contained their original defects increased in size proportional to the increase in layer thickness. Hence, while it seems possible to avoid the growth of these defects and obtain GaP layers of good structure on GaAs substrates, it is not likely that defects once formed can be healed.

The beneficial effect of the pretreatment in phosphorus-hydrogen may be three-fold. First, the surface is cleaned of oxide impurities; second, the pressure of phosphorus prevents the GaAs from undergoing decomposition; and third, a starting epitaxial GaP surface is formed by diffusion.

Data on deposition runs using the pretreatment in phosphorus vapor at 1000° C are summarized in Table I. The gallium source temperature for all runs was 890° C except for runs SC 12 and SC 13 for which it was 935° C.

The phosphorus flow rates are averages calculated from the total weight loss. Actual rates probably ranged from 4 cc/min down to as low as 1 cc/min during the course of the longer runs. For runs SC 12 and SC 13, in which a GaP source was used, the phosphorus rates given in parentheses are those during the pretreatment period only. The flow of excess phosphorus was discontinued during deposition.

the surface defects is not clear. However, as discussed above, the incidence of bumps of the type shown in Figures 8 and 9 is greatly reduced or virtually eliminated by the high temperature phosphorus treatment even in cases where a ragged interface is formed (SC 5, Figure 12 and SC 9, Figure 11). Most bumps which form during a normal run are of a uniform size and therefore probably were nucleated at the GaAs surface. Occasionally, however, as on SC 6-3, a few small or medium sized bumps may be discerned which must have nucleated on the surface of the growing layer. Again, evidence is found, as in SC 10 (Figure 10), that a disturbance in growth conditions can cause a severe bump formation even after a smooth growth surface has presumably been initiated. That the substrate material may affect bump formation is indicated by run SC 12 in which the Hall bar surfaces were smooth, while the wafers, cut from different material, were covered with small sharp bumps. Finally, the failure of runs SC 12 and SC 13 to produce smooth layers may implicate a low phosphorus pressure, an excess not being used, although the change in temperature profile (in unsuccessful attempts to increase growth rate) may be responsible.

In one preliminary experiment in which < 111 > oriented substrates were included, the growth rate on the < 111 > surfaces was only about one fourth that on the < 100 >. In addition, a considerable amount of polycrystalline nodular growth occurred on the < 111 > face. However, except for this polycrystallinity which might be eliminated by the high temperature treatment in phosphorus vapor, and a series of growth steps due to a small deviation from the < 111 > orientation, the surfaces were excellent. Potentially, therefore, superior growth may be attained in the < 111 > direction.

Pending discovery of conditions for rapid growth to achieve thick layers of GaP, one wafer about 175 microns thick was grown by repeated deposition on the same GaAs substrate (Runs SC 6 through SC 11) followed by etching in concentrated nitric acid to remove the substrate. As shown in Figures 15 and 16 the top surface of the wafer is very irregular, caused by accumulation of all the defects of the six depositions aggravated by failure of the cleaning procedure in the presence of bumps. The bottom surface, except for a slight etch figure greatly exaggerated in Figure 17, is smooth and flat. The etch pattern resembles wipe

Substrate positions are those of the wafers except for AP89D where the position of the one fresh Hall bar is given. These positions may be compared with the zone of maximum deposition ("dump" zone) on the wall which occurs between 13" and 14" to 15".

Approximate layer thicknesses are derived from measurements [2] on Hall bars which were located adjacent to the wafers during deposition. The growth rates given for the four runs in which the HCl flow rate was doubled during the course of the run refer to the higher flow rate. For calculation the growth rate during the initial low flow rate period was assumed to be one half of that during the remaining time.

The data indicate that growth rate increases as the wafer is moved into the "dump" zone, and increases with overall increase in flow rate. However there is a decrease in growth rate if the HCl flow is increased without a corresponding increase of the hydrogen flow (Runs SC 6 and SC 7). Because of the varying interface and surface conditions, however, these deductions cannot be considered conclusive.

Sections cleaved from Hall bars (or wafers) are shown in Figures 2 through 7 to illustrate the degree of raggedness as listed under "Interface" in Table I. Referring to the notes it may be seen that the ragged interfaces are related to conditions under which the GaAs substrate could be etched prior to or during initial GaP deposition. Smooth interfaces (excepting run SC 12) were obtained when care was taken to preheat the phosphorus before raising the substrate temperature to a high value. Extreme raggedness resulted in the one run (SC 5) in which relatively impure phosphorus was used and in the run (SC 4) in which the substrate was heated above the decomposition temperature of GaAs before initiating phosphorus flow. The varying degrees of irregularity of the other runs probably reflect the condition of the phosphorus charged. SC 12 was run at a higher temperature and etching may have occurred during the initial deposition. It has been observed previously under similar conditions that simultaneous etching of GaAs and growth of GaP do take place.

A variety of surface defects found on the < 100 > growth planes are shown in Figures 8 through 14. In contrast to the interface irregularity, the origin of

marks and may be due to the distribution of residue after final wiping of the substrate.

The method of substrate removal eliminates the problem of maintaining parallelism and the danger of introducing work damage into the GaP layer which would accompany a lapping technique, and thus makes available for device fabrication the thin layer of GaP adjacent to the interface. The structure of this layer might be optimized by slow growth before applying a thick supporting layer of poorer structure at a rapid rate.

B. Electrical Properties

Electrical properties of epitaxial GaP wafers, including five previously prepared samples, which have been made available for testing solar cell fabrication techniques, are listed in Table II. All of the epitaxial layers were N type without deliberate doping. The electrical properties are averaged from measurements on Hall bars which are located adjacent to the wafer during deposition. Hall bars are cleaved from polished slices of high resistivity GaAs. The values reported for samples through AP 88-5 are of questionable significance due to difficulties in obtaining electrical contacts. Wide discrepancies between Hall bars in the same run, for example in AP 60 and AP 62, and high mobilities are suspect. Data for sample SC 4-3 and below were obtained using contacts of pure indium alloyed at 700-800° C in hydrogen using a strip heater. Consistent results have been obtained in all runs except SC 13 in which ohmic contacts, for reasons not yet explained, did not form.

On comparing the data of Table II with that of Table I, a possible correlation of carrier level with growth rate is observed for runs using the same source material and temperature profile (SC 4 through SC 11). The correlation is plotted in Figure 18. In view of the variables involved and uncertainty in determining both values, the correlation is not bad.

A strong impurity segregation accompanying GaP deposition is indicated by the trend in carrier level derived for successive Hall bars in the same run. The data for individual Hall bars are tabulated in Table III. In these heavily compensated materials there is, as expected, no significant effect on mobility.

IV. SOLAR CELL FABRICATION

A. Diffusion

Since the epitaxial deposits were N type, P type dopants were diffused to form P-N junctions. Zinc is known to give rise to a relatively shallow acceptor level [3] and to have a suitable solubility and diffusion constant in GaP[4] to be used for producing P-N junctions.

Since so little is known about the properties of GaP, initial efforts were directed toward gaining more information on the general problems connected with P-N junction fabrication including surface concentration, diffusion time, junction depth, junction front and junction delineation techniques. Further, because solar cell design is a compromise between optimizing bulk phenomena and minimizing surface effects, additional emphasis was placed on studying junction depth.

The initial experiments were conducted in closed tubes approximately 20 ml in volume using various zinc sources including pure zinc (99.999%), zinc arsenide and zinc with added phosphorus. The samples which consist of epitaxial GaP on GaAs substrates rest in the closed tube on quartz shelves. The zinc source is placed in a graphite boat which is placed under the quartz shelf. Necessary preliminary steps to minimize the contamination from the graphite boat were taken. This includes cleaning the boat in boiling HNO_3 followed by a rinse and then baking in vacuum (10^{-4} mm) for 30 minutes at 900° C to 1100° C. The quartz capsule and plate are boiled in HNO_3 for one hour and rinsed in deionized H_2O and dried with dry nitrogen. The epitaxial samples are cleaned in an ultrasonic bath for 3 minutes in absolute alcohol and 5 minutes in undiluted reagent grade H_2SO_4. This is followed by five thirty-second rinses in distilled water. The water is poured off and replaced by alcohol. The sample is removed from the alcohol bath, just prior to placing it in the diffusion capsule and wiped dry with lens tissue. It is then placed on the silica plate in the diffusion tube,

the diffusant source placed in the graphite boat, and the entire apparatus evacuated to 5×10^{-7} mm Hg and sealed off. The diffusion tube is placed in a preheated furnace for a desired time, then removed to the edge of the furnace for a short time and then removed from the furnace and allowed to cool to room temperature, whereupon the samples are removed and tested.

In Table IV are listed the run number, slice number, the P type source material and the amount used, the diffusion temperature and time, the average surface concentration after diffusion (P type) and the resultant carrier mobility. These were determined from Hall effect and electrical resistivity measurements at room temperature. The last column lists the junction depth determined by junction delineation techniques to be discussed below.

In each case reported it was possible to make P-N junctions using the zinc diffusion procedure. The temperatures generally were between 800 and 850°C although a few samples have been diffused at higher temperature. The 800 to 850° C range was found to give better control for shallow junctions and to reduce the occurrence of zinc alloying.

The epitaxial layers used so far have not had good structure as shown above. Figure 19 shows a cleaved section of one of the early epitaxial deposits after zinc diffusion and etched to delineate the P-N junction. The junction is very ragged with diffusion spikes at an angle which suggests they are parallel to stacking faults.

Attempts to improve the junction quality by carrying out the zinc diffusion in the presence of added arsenic or phosphorus has led to some improvement in the junction front. In addition, the junction depths are somewhat shallower.

A zinc diffusion has been carried out in only one of the layers prepared by pretreating the substrate with phosphorus (SC5-3). In spite of the absence of any visible defects of a high frequency along the cleaved edge (Figure 13) the P-N junction does exhibit a number of spikes or fingers extending below the junction plane. In several other samples having smooth surfaces, however, many very faint lines in the surface perpendicular to the cleaved edge have been discerned (see, for example, SC12-7, Figure 14). These may correspond to defects of a type down which rapid zinc diffusion may occur, and may account for the non-planarity of the diffused P-N junctions.

The surface concentrations as deduced from room temperature Hall effect measurements and known junction depths are found, using the diffusion conditions noted in Table IV and discussed above, to vary from about 4.5×10^{18} to about $1.6 \times 10^{19}/cm^3$. The corresponding hole mobility is about 30 cm^2/volt sec.

B. Junction Delineation

The following procedure has been used for delineating the P-N junction formed by zinc diffusion:

The single crystal epitaxial layers which are generally grown in the $< 100 >$ or $< 111 >$ orientation are cleaved and delineated by etching in conc. (48%) HF for about 3 minutes at room temperature under the influence of light (an American Optical microscope lamp can be used). Following the etching action the samples are rinsed in H_2O and alcohol and then mounted on an object slide with plasticine and leveled to bring the cleavage plane exactly at right angles to the optical axis of the microscope. The junction depth is measured directly with an optical microscope equipped with incident lighting, a stable mechanical stage and a calibrated eyepiece scale. Measurements are usually made at magnifications of 500 diameters.

Another etch that may be used is the copper stain etch consisting of 10 gms $CuSO_4$ and 0.3 ml HF in 100 ml H_2O. The etching is also carried out in the presence of light.

C. Contacts to P and N Faces

Following the diffusion cycle, the back side of the wafer is lapped back to remove the diffused zinc. Since N type GaAs substrates have been used as supports for the epitaxial layer, a 50%-50% AuSn alloy is evaporated onto this substrate followed by evaporated nickel. The sample is then placed in a tube in a furnace where it is evacuated and then flushed with argon. The alloying is carried out at $\sim$ 550° C in an argon atmosphere.

The contact to the diffused P type face is made by evaporating silver through a mask onto the specimen heated to $\sim$ 200° C.

Similar procedures have been used on bulk GaP.

D. Etching

The cells have generally been etched with aqua regia with the contacts masked. The etch has generally improved the short circuit current density (at room temperature) and has been found to be controllable.

V. EVALUATION

A. Solar Cell Characteristics

Room temperature measurements of the open circuit voltage (V_{oc}) and short circuit densities (J_{sc}) of the fabricated cells were routinely measured using a tungsten source calibrated with a silicon solar cell for a 100 mw/cm^2 output. The tungsten source temperature was 2800° K. Cell voltage was measured with a Model No. 31 Cary electrometer and current with a HP Model No. 425A D. C. microvolt ammeter.

The results of the measurements are shown in Table V, where the values are given both initially and after etching with aqua regia. Highest open circuit voltage was obtained with epitaxial sample AP 62-2 with a value of 0.75 volts. The best obtainable short circuit current density thus far has been 0.23 ma/cm^2 also found with cell AP 62-2. Cell areas ranged from about 0.02 cm^2 to about 0.2 cm^2.

The variable and generally low values of V_{oc} are attributed to the rather poor junctions formed in the gallium phosphide that has been prepared so far.

From theory,[5-9] the open circuit voltage is given approximately by

$$V_{oc} \sim \frac{kt}{e} \ln \left[\frac{J_L \; D_p \; n_n}{2.23 \times 10^{31} \; T^3 \; e \; L_p} \; \epsilon^{-Eg/kt} \right]$$

Where J_L is the generated short circuit current density, D_p, L_p are the carrier diffusion coefficient and length (it is assumed that $D_p = D_n$; $L_p = L_n$), n_n is the carrier density of the N type material, Eg is the energy gap, T, the absolute temperature. The effective masses have been taken equal to the free electron mass. For GaP, the following values are assumed: $J_L = 10$ ma/cm^2, $D_p = 2$ cm^2/sec, $L = 10^{-5}$ cm, $T = 300°$ K, $Eg = 2.25$ e.v., $n_n = 10^{17}$/cm^3. With these values an open circuit voltage of about 1.5 volts is expected at room temperature.

However, in spite of the large variation in V_{oc} between the samples and aside from those where there are obvious shorting effects, there is at most a factor of three between the values obtained and that expected theoretically.

On the other hand, the best values of short circuit current density, J_{sc} obtained are only about 0.2 ma/cm^2.

Ideally for GaP, from the maximum rate of carriers generated by solar radiation at the absorption edge of GaP (9.6×10^{16}/cm^2/sec) and with 100% collection efficiency a short circuit current density of 15 ma/cm^2 might be expected. From the relationship of Moss [6]

$$\frac{J_{sc}}{e\,\Phi} = \frac{K L \left[\alpha + KL - (1+\alpha)\exp(t/L - Kt)\right]}{(K^2L^2 - 1)(\cosh L/l + \alpha \sinh L/l)} = Q \text{ (collection efficiency)}$$

where J_{sc} is the short circuit current density, e is the electron charge, Φ is the number of photons generated per second per cm^2, K is the absorption coefficient, L is the carrier diffusion length (hole and electron diffusion lengths are assumed equal), t is the thickness of the P layer, and α as a surface recombination factor, one can, by assuming appropriate values for Kt, KL ($Kt < KL$, $KL \sim 1$) and neglecting surface recombination ($\alpha = 0$), estimate a collection efficiency at room temperature of 50%. The short circuit current density is then 7 ma/cm^2.

The expected values for J_{sc} of about 7-15 ma/cm^2 is about 35 to 75 times larger than the present observed values.

Grimmeiss and coworkers [10] have reported short circuit currents of up to 5 ma/cm^2 and open circuit voltage of up to 1.2 volts in zinc-diffused single crystal gallium phosphide photovoltaic cells.

During this initial period some experiments were carried out with bulk polycrystalline material. The processing of the bulk material (N type) for solar cell fabrication was similar to that described for the epitaxial samples with the exception that the surface of the bulk samples were polished prior to the diffusion. Results on the bulk samples are found in Tables IV and V and are identified under "slice number" where they are listed as polycrystalline ingots. They can be further identified from the diffusion treatment. Because of the polycrystalline

nature of the samples the delineation technique could not readily be used to determine junction depths. The highest open circuit voltage yet obtained experimentally has been found with NA-7 which had a value of 1.0 volts. However, as before, the short circuit current density is low. Since the bulk material was polycrystalline, grain boundaries, etc. could be influencing the characteristics.

Thus far the best room temperature efficiency attained for GaP solar cells in the present program has been $\sim .1\%$.

The data and observations presented thus far point up the rather low value of the short circuit current density obtained at room temperature both for single crystal GaP epitaxially deposited on GaAs and for bulk polycrystalline GaP. Attempts to vary the junction depth from 0.5 μ to 16 μ have produced no consistent picture on the short circuit current density. All diffusion depths from very shallow to deeper produce low short circuit current densities. Some variation and improvement is made with etching but the upper limit appears thus far to be .2 ma/cm^2 at room temperature.

From the simplest considerations, neglecting surface recombination, reflection losses, etc., the short circuit current may be expressed by a highly idealized relation

$$J_{sc} \approx e \Phi K L$$

where e is the electronic charge, Φ is the maximum number of photons generated by solar radiation at the absorption edge of GaP (approx. 9.6×10^{16} /sec/cm^2), K is the absorption coefficient at the band edge and L is the minority carrier diffusion length. For an observed J_{sc} of .2 ma/cm^2, KL is 0.013 ($<< 1$) and if K is 100 cm^{-1}, L is about 1.3×10^{-4} cm. Estimating the carrier diffusion coefficient from a carrier mobility of about 100 cm^2/volt sec and the Einstein relation, $\mu/D = e/kt$, $D = 2$ and the minority carrier lifetime is about 10^{-8} sec.

The generally short lifetimes are in accord with those reported in GaP by Gershenzon and Mikulyak [3] (about 10^{-10} sec. for injected carriers at low bias) and the workers at the Westinghouse Research Laboratories [12] (about 10^{-12} sec.).

B. Sheet Resistance and Surface Concentration

The sheet resistance of the epitaxial samples listed in Table IV has been found to vary from about 10 ohms (NA-11, AP 88-2) to about 100 ohms (NA-1, AP 62-2). As expected, a variation with surface concentration is noted. However,

it is al so noted that the open circuit voltages generally vary with the surface concentration. Lower surface concentration generally show higher open circuit voltages. It is possible that this latter result may be related closely to the poor junction fronts, fingers and spikes noted previously.

C. Spectral Response

Spectral response of the cells was measured at room temperature with a Bausch and Lomb grating monochromator with a grating blazed for 2 microns first order. Calibration of the monochromator intensity is awaiting receipt of another grating blazed for 5 microns. The short circuit current was measured with a Hewlett Packard D. C. Microvolt ammeter, Model 425A. A typical spectral response curve for the GaP cells is shown for sample NA-13, bulk sample.

The spectral response peaks are shown in Table V. The primary peak is found to occur at a wavelength from 0.46 to 0.54 micron in agreement with the photovoltaic data of Grimmeiss and coworkers [10]. A secondary peak also reported by Grimmeiss and coworkers is found for some of the samples at about 0.7 micron. Not all the samples show such a secondary peak. In Table VI are given, for the cells of Table V, the relative ratio of the response of the secondary peak to the primary peak. It will be noted that the secondary peak response is generally small compared to the primary peak except in the case of NA-10, bulk polycrystal, where the ratio approaches 1/2. The epitaxial samples generally show only a small response in the .70 μ region.

From spectral response data for NA-1, AP 62-2, using the relation of Lamond and Dale [13]

$$\frac{I_{p_1}}{I_{p_2}} = \frac{1 + \dfrac{1}{\alpha_2 L_p}}{1 + \alpha_1 L_p} \exp\left[- X_j (\alpha_1 - \alpha_2)\right]$$

where I_{p_1} is the current at the peak response wavelength, I_{p_2} is the current for wavelength of half peak response, α_1, α_2 are the absorption coefficients at these points, X_j is the junction depth, L_p is the diffusion length, one obtains a diffusion length of about 0.8×10^{-4} cm.

Assuming a carrier diffusion coefficient of 2 cm^2/volt sec. one finds a lifetime of 3.3×10^{-9} sec. which again is in fair agreement with the estimates

based on the short circuit current density.

It is interesting to note from the data in Table VI that there is some correlation between higher short circuit current and higher ratio of low energy response to high energy response in the epitaxial samples. Gershenzon and Mikulyak [3] have suggested that photoluminescence and electroluminescence emission in gallium phosphide around 0.7 micron is associated with recombination through a deep donor level about 0.4 e.v. below the conduction band and that this level is due to oxygen impurity. They further pointed out that gallium phosphide prepared by open-tube methods does not exhibit photoluminescence or electroluminescence and this was attributed to low concentration of oxygen impurity and hence of the deep donor center. If the photoresponse of the photocell in the region of 0.7 micron is associated with transitions from the valence band to the deep donor level, the correlation noted above would suggest that increased oxygen content in the gallium phosphide would improve the short circuit current. However, it is difficult to postulate a plausible mechanism.

D. Effects of GaP-GaAs Interface

The necessity of presently working with thin epitaxial layers of gallium phosphide on gallium arsenide substrate has led to consideration of the GaP-GaAs interface. The photovoltaic effect of this heterojunction due to absorption of light transmitted by the GaP layer would be to oppose the photovoltaic effect of the GaP P-N junction. To test the effect of the heterojunction an experiment was conducted with an epitaxial specimen consisting of N GaP (35 μ) on N^+ GaAs. An In-Sn-gold Kovar disc was alloyed into the N^+ GaAs substrate and a gold dot (.025 cm dia.) was evaporated on the GaP. The open circuit voltage was observed under a tungsten source and with the setup previously described to be 0.9 volt with the polarity opposite to that expected for the heterojunction (that is, the gold dot was positive and the Kovar disc negative). This potential was therefore primarily that of the photo response of the GaP-Au barrier. A portion of the surface of the GaP including the gold dot was covered with black wax and the sample remeasured. The open circuit voltage was reduced but the polarity remained the same. With black wax completely covering the surface and sides, the open circuit voltage was reduced to about 60 millivolts and the polarity was unchanged.

It appears from this experiment that the effect of the GaP-GaAs interface in this sample on the solar characteristics is small. However, the rather ragged GaP-GaAs interface in this specimen may account for the small photoresponse of the interface.

E. Junction Characteristics

A typical 60 cycle I-V trace of a fabricated cell is shown in Figure 21. The reverse characteristic is poor with a large reverse current appearing above about 0.4 volts. The forward trace exhibits a forward drop which is lower than would be expected for GaP. The characteristic is consistent with the poor appearance of the junction.

Static D.C. forward current-voltage characteristics of these cells gave for n in the equation $I = I_o \exp ev/nkT$ values between 2 and 4 which suggests from the work of Sah, Noyce and Shockley [11] that the forward current is a result of recombination within the junction region.

Gershenzon and Mikulyak [3] have reported anomalies in gallium phosphide diffused junctions, characterized primarily by a nearly compensated layer right at the junction as deduced from the junction resistance and the reverse-bias junction capacity. As a prelude to similar measurements in the present work the effects of heat treatment (simulating the zinc diffusion schedule) on the gallium phosphide prior to diffusion were investigated. The study was carried out on 3 representative samples, NA-1, AP 62-2 (epitaxial), NA-4 bulk polycrystalline and NA-5, AP88-5 (epitaxial). The carrier concentrations were deduced from capacity-voltage data. For the initial case, Hall data was also available for the two epitaxial samples. A comparison of the carrier concentration was made on samples before and after the heat treatment simulating the zinc diffusion cycle (800° C for 3 minutes). In addition, these results were compared with the samples which had zinc diffused and P-N junctions formed and from which mesas were made and capacity-voltage measurements carried out. In the first two experiments In-Sn-Au Kovar discs were alloyed on the back side and gold dots ($\sim$.025 cm dia) evaporated on the front.

The samples could generally be characterized by a $\frac{1}{C^2}$ vs V relationship, especially as the space charge region extended deeper into the bulk as can be seen by the capacity-voltage curves given in Figure 22-24 for the three samples discussed. The grid on which the data is portrayed is described by

the relationship

$$C/A = 2.5 \times 10^{-4} \left(\frac{N_D}{V_i - V} \right)^{1/2} \quad pf/cm^2$$

where C is the capacity in picofarads, A is the area of the gold dot or junction, N_D is the net number of ionized donors, V_i is the built in voltage for N type GaP (taken as 1.3 volts), V is the applied reverse voltage.

One of the exceptions to the above $1/C^2$ - V relationship was found for the mesa of sample NA-4, bulk polycrystalline material. It was thought that surface effects in this case may be playing a more prominent role than for the other cases and hence be responsible for the deviation from the $1/C^2$ law. As the space charge region went deeper into the material below the surface there were indications that the $1/C^2$ vs V law might hold here too. The results of the experiment are shown in Table VII. Incidentally, reasonably good agreement was obtained for the initial material when comparing the Hall effect (average) and the C-V data.

It is noted from Table VII that, in the case of the epitaxial samples, within experimental error and homogeneity of the samples, little or no change in carrier concentration results in heat treatment or with the zinc diffusion. The case for the mesa polycrystalline bulk sample, NA-4, was somewhat confusing especially since the heat treatment did not show any large change in carrier concentration and it was believed that the initial deviation from the $1/C^2$ law and the fact that the deviation from the $1/C^2$ law occurred less than 1 μ from the surface with zinc diffused in might be construed as "surface" effects. The measured values of short circuit current density (taken from Table V and reproduced) do not bear out any great differences in these samples.

To further supplement the above measurements and at the same time test whether the results on NA-4 after diffusion was a real effect, D.C. I-V characteristics were taken in the forward direction and the series resistance at high forward current as well as the values of I_o and n in the relationship $I = I_o \exp ev/nkT$ were calculated. These are given in Table VIII. It can be seen that there is no anomaly in these samples. They are, aside from the values for I_o, in good agreement with each other. There are no great differences in series resistance and no high values as reported by others [3, 12]. The values are

about .02 ohm cm^2 which is lower than the 1 ohm cm^2 reported [3, 12]. It is possible that the low values of series resistance observed in these epitaxial samples prepared by the open tube process may reflect the absence of the deep donor (0.4 e.v.) attributed to oxygen by Gershenzon and Mikulyak [3] and suggested as the compensating impurity that gives high resistance junctions.

However, the saturated current (I_o) in the present junctions are generally many orders of magnitude higher than the theoretically predicted values so better junctions are required before conclusions can be drawn.

VI. CONCLUSIONS

Good epitaxial interfaces of gallium phosphide on gallium arsenide have been achieved only after high temperature treatment of the initial gallium arsenide surface with hydrogen and phosphorus which cleans the surface or phosphides the gallium arsenide to some degree, or both. Prolonged growth periods are required to grow gallium phosphide layers sufficiently thick to be self supporting. The layers that have been prepared contain defects which result in "spikes" and non-planar junctions formed by zinc diffusion. These defects may be associated with stacking faults which generally arise from dirty or imperfect substrate surfaces.

The poor quality of the junctions is also evident in large leakage currents when biased and in somewhat low values of the open circuit photovoltage.

The low short circuit photo currents that have been observed are attributed to short lifetime of minority carriers, the reasons for which are as yet obscure.

VII. FUTURE STUDIES

The efforts to grow thick layers of GaP will be continued by modification to permit longer deposition time.

Techniques to eliminate from the critical region of the layer all defects, particularly those leading to non-planar P-N diffusion junctions must be perfected. Several approaches may be effective and will be attempted as time permits, including (1) improvement of the cleaning procedure, (2) further purification of the reaction gases, and (3) increase of the phosphorus pressure.

The impurity level of the gallium phosphide must be brought under control. To this end, in addition to the steps listed above, (1) different sources

of gallium and phosphorus will be tried, (2) methods of controlled doping with selenium and tellurium must be developed, (3) the effect of doping with oxygen, alone or in combination with other impurities should be established.

Work on improving the junction quality by modifications of the diffusion conditions and optimization of junction depth will be continued. Measurements of the optical properties of gallium phosphide single crystals will be initiated and the monochromator will be calibrated. Measurements of the solar cell characteristics at elevated temperature are planned.

VII. REFERENCES

1. F. V. Williams and R. A. Ruehrwein, J. Electrochem. Soc., 108, 177C (1961).
2. A. H. Herzog, Semiconductor Products, p. 25, Dec., 1962.
3. M. Gershenzon and R. M. Mikulyak, J. A. P., 32, 1338 (1961); Solid State Electronics, 5, 313 (1962).
4. Chang and Pearson, Stanford Quarterly Research Review, No. 1, SE 1-62-109, p. 78-81, Stanford Electronics Laboratories.
5. M. B. Prince, J. A. P., 26, 534 (1955); M. Wolf, Proc. IRE, 48, 1246, (1960).
6. T. S. Moss, Solid State Electronics, 2, 222 (1961).
7. J. J. Loferski, J. A. P., 27, 777 (1956); Proc. IEEE, 51, 667 (1963).
8. P. Rappaport, RCA Rev. 21, 373, (1959).
9. D. A. Kleinman, B. S. T. J., p. 85, 1961.
10. H. C. Grimmeiss, A. Rabenau and H. Koelmans, J. A. P., 32, 2123 (1961).
11. Sah, Noyce and Shockley, Proc. IRE, 45, 1228 (1957).
12. Final Report, Report No. 4, DA 36-039 SC-88889, Westinghouse Electric Corp., Central Research Laboratories.
13. P. Lamond and B. Dale, Colloque International sur les dispostifs a' semiconducteurs, Paris, Vol. 1, p. 635 (1961).

TABLE I

Epitaxial Deposition of GaP on GaAs Substrate

Run No.	Time (Minutes)	Flow Rates (cc/min) HCl	H_2	P_4	Substrate Position (inches)	Substrate Temp. ° C	Layer Thickness (Microns, approx)	Growth Rate (μ/min)
AP89D	60	1	150	1.9	16-1/2	800	5	.08
SC4	75	1	150	1.8	16	800	8	.11
SC5	60	1	150	1.8	16	800	13	.22
SC6	15 157	1 2	150 150	1.7	15-1/4	805	10	.061
SC7	15 239	1 2	150 150	1.8	14-1/2	810	19	.077
SC8	15 118.5	1 2	150 300	2.1	14	815	40	.32
SC9	60	1	150	3.8	14	815	14	.23
SC10	60 101	1 2	150 300	2.5	14	815	49	.37
SC11	240	1	150	2.1	14	815	43	.18
SC12	720	1	150	(1.8)	14-1/2 15-1/2	870 860	24	.033
SC13	258	1	150	(2.8)	15 16	830 815	40	.16

TABLE I (Cont'd)

Epitaxial Deposition of GaP on GaAs Substrates

Run No.	Interface	Surface	Remarks
AP89D	very slightly ragged	smooth	(2)
SC4	very ragged	bumps	(1)
SC5	extremely ragged	bumps, poly	(3), (6)
SC6	very slightly ragged	few bumps	(4), (7)
SC7	slightly ragged	many bumps	(4)
SC8	ragged	many bumps	(4)
SC9	smooth	smooth	(5)
SC10	smooth	covered with bumps, poly.	(5), (8)
SC11	smooth	smooth	(5)
SC12	slightly ragged	wafers covered with small sharp bumps. Hall bar smooth	(5), (9)
SC13	smooth	covered with bumps	(5), (9)

(1) Heated to 1000° C before phosphorus source brought to temperature.

(2) Heated to above 800° C before phosphorus source brought to temperature.

(3) Heated to 800° C before phosphorus source brought to temperature.

(4) Heated to 760° C before phosphorus source brought to temperature.

(5) Heated to 400° C before phosphorus source brought to temperature.

(6) Fisher P-99 phosphorus source.

(7) Freshly degassed phosphorus, L. Light, red, 5N.

(8) Outlet plugged by condensing phosphorus during run causing wide fluctuation and flow rates and pressures.

(9) GaP source, phosphorus flow discontinued after starting HCl flow.

TABLE II

Properties of GaP Epitaxial Layers (N Type)

Sample No.	Source	Thickness, μ (approx.)	ρ	μ	n	Remarks
AP48-2	Ga + P	7	.12	280	3.0×10^{17}	
AP49-2	"	2.5	.021	110	4.3×10^{18}	
AP60-2	GaP	38	.057	100	2.2×10^{18}	
			6.4	80	1.2×10^{16}	
AP62-2	"	13.5	3.5	335	6.4×10^{15}	
			0.22	400	1.5×10^{17}	
AP62-4	"	15	0.22	400	1.5×10^{17}	
			3.1	63	3.4×10^{16}	
AP87-2	GaP + GaAs	35	.032	110	2.0×10^{17}	Graded interlayer
AP88-2	"	9	.14	180	5.0×10^{17}	Graded interlayer <111> orientation
AP88-5	"	35	.83	140	5.7×10^{16}	Graded interlayer
SC4-3	Ga + P	9	.14	75	6.8×10^{17}	P-type substrate wafer
SC5-3	"	13	1.0	81	1.4×10^{17}	" " "
SC6-3	Ga + P	10	2.65	68	3.5×10^{16}	Deposition repeated
SC7-3	"	19	1.37	53	1.7×10^{17}	on same water.
SC8-3	"	40	.299	81	2.9×10^{17}	Evaluations made
SC9-3	"	14	.386	72	2.8×10^{17}	on fresh Hall bars
SC10-3	"	49	.110	82	7.2×10^{17}	each run.
SC11-3	"	43	.651	93	1.3×10^{17}	
SC6/11		175 Total	.250	80	3.4×10^{17}	Averages
SC12-4	GaP	27	1.13	53	2.0×10^{17}	
SC12-6	GaP	30	7.2	48	4.2×10^{16}	
SC13-4	GaP	40	-	-	-	non-ohmic contacts
SC13-6	GaP	40	-	-	-	non-ohmic contacts

TABLE III

Carrier Level and Mobility vs Hall Bar Position

Run No.	Hall Bar	Carrier Density			Mobility		
		1st	2nd	3rd	1st	2nd	3rd
SC4		7.0×10^{17}	6.7×10^{17}		72	78	
SC5		1.7×10^{17}	1.0×10^{17}		49	113	
SC6		3.5×10^{16}	-		68	-	
SC7		2.8×10^{17}	5.8×10^{16}		55	51	
SC8		3.6×10^{17}	2.2×10^{17}		92	71	
SC9		3.8×10^{17}	1.7×10^{17}		79	65	
SC10		8.6×10^{17}	5.7×10^{17}		80	85	
SC11		1.9×10^{17}	7.0×10^{16}		92	95	
SC12		3.2×10^{17}	7.5×10^{16}	1.0×10^{16}	61	45	51

TABLE IV

Solar Cell Fabrication

Diff. Run No.	Slice No	Diffusant Source and Amt.	Diff Temp. (°C)	Diff Time (min)	P Surface Conc/cm^3	μ Of P Layer cm^2/volt sec	Junction Depth μ
NA-1	AP62-2	3.8 mg Zn_3As_2	800	3	4.7×10^{18}	48	1
NA-2	AP62-4	2.2 mg Zn	800	10	4.5×10^{18}	31	5
NA-3	AP48-2	2.2 mg Zn	800	3	-	-	3
NA-4	AP87-2	2.2 mg Zn	800	3	7×10^{18}	27	2
NA-4	bulk, poly	2.2. mg Zn	800	3	-	-	
NA-5	AP88-5	5.8 mg Zn	800	3	1×10^{19}	28	2
NA-6	AP60-2	2.2 mg Zn	850	1.5	-	-	$< 1 \mu$
NA-7	SC5-3	5.8 mg Zn	850	2.5	1.3×10^{19}	23	2
NA-7	bulk, poly	5.8 mg Zn	850	2.5	-	-	-
NA-8	bulk, poly	5.8 mg Zn	800	30	-	-	16 (est. from spectral resp.
NA-9	bulk, poly	30% Zn, 70% Ga 14.7 mg Zn, 34.3 mg Ga	1000	3	-	-	-
NA-10	bulk, poly	5.8 mg Zn, 1.8 mg P	800	3	-	-	-
NA-11	AP88-2	5.8 mg Zn, 1.8 mg P	800	3	1.6×10^{19}	-	0.6
NA-11	bulk, poly	5.8 mg Zn 1.8 mg P	800	3	-	-	-
NA-12	AP49-2	30 mg Cd	827	10	-	-	$< 1 \mu$
NA-12	bulk, poly	30 mg Cd	827	10	-	-	-
NA-13	bulk, poly	5.8 mg Zn, 1.8 mg P	800	10	-	-	-

TABLE V

Solar Cell Evaluation

Diff. Run No.	Slice No	Before Etch V_{oc} volts	Before Etch J_{sc} ma/cm^2	After Etch V_{oc} volts	After Etch J_{sc} ma/cm^2	Spectral Response Peaks, Microns Main	Spectral Response Peaks, Microns Secondary
NA-1	AP62-2	.73	.19	.76	.23	.46	.70
NA-2	AP62-4	.53	.11	.74	.19	.49	.70
NA-3	AP48-2	---------- Sample Shorted Out ----------					
NA-4	AP87-2	.40	.04	.56	.12	.47	.70
NA-4	bulk, poly	.67	.09	.96	.19	.46	.70
NA-5	AP88-5	.44	.10	.52	.14	.47	-
NA-6	AP60-2	-------- Surface Resistance too high - contacts poor ----------					
NA-7	SC5-3	-------- P-type Substrate - No solar cell made ----------					
NA-7	bulk, poly	.80	.016	1.0	.069	-	-
NA-8	bulk, poly	.10	.016	.10	.022	.49	-
NA-9	bulk, poly	.23	.06	.08	.067	.54	.70
NA-10	bulk, poly	.03	.14	.27	.05	.49	.70
NA-11	AP88-2	.003	.065	.02	.123	.45	-
NA-12	AP49-2	.00	.05	.00	.015	.46	.72
NA-12	bulk, poly	.03	.024	.08	.018	.54	.70
NA-13	bulk, poly	.06	.054	.14	.08	.50	.67

TABLE VI

Run No.	Sample No.	$\frac{I_{\lambda \text{ sec. peak } (\sim .7\mu}}{I_{\lambda \text{ pri. peak (band edge)}}}$	μ (cm^2/volt sec)	J_{sc} (ma/cm^2)	Series Resistance $R_s A$ (ohm cm^2)
NA-1	AP62-2	4/166	370	.23	17.3×10^{-3}
NA-2	AP62-4	9/117	230	.19	-
NA-11	AP88-2	0/185	175	.123	-
NA-5	AP88-5	0/161	137	.14	18.3×10^{-3}
NA-4	AP87-2	1/215	106	.12	-
	Bulk Samples				
NA-4	bulk, poly	16/145	-	.19	15.6×10^{-3}
NA-11	"	0/155	-	.14	-
NA-10	"	91/184	-	.11	14.6×10^{-3}
NA-13	"	47/230	-	.08	-
NA-9	"	18/136	-	.07	-
NA-12	"	8/242	-	.024	-
NA-8	"	0/212	-	.022	-

TABLE VII

Variation in Carrier Concentration of Sample with Heat Treatment

Sample	Carrier Concentration From Hall Effect (no/cm^3)	Carrier Concentration From C-V Data (no/cm^3)	Mesa Area (cm^2)	Short Circuit Current Density J_{sc}
A				
NA-1, AP62-2	7.8×10^{16}	3×10^{16}	-	-
NA-4, bulk, poly	-	1×10^{17}	-	-
NA-5, AP88-5	5.7×10^{16}	5×10^{16}	-	-
B				
NA-4, bulk, poly	-	3×10^{16}	-	-
NA-5, AP88-5	-	1×10^{16}	-	-
C				
NA-1, AP62-2	-	1×10^{16}	1.75×10^{-3}	.23 ma/cm^2
NA-4, bulk poly	-	7×10^{14}	2.6×10^{-3}	.19 ma/cm^2
NA-5, AP88-5	-	9×10^{16}	3×10^{-3}	.14 ma/cm^2

A - Starting material before diffusion or heat treatment.

B - Samples heat treated at 800° C - (simulating diffusion schedule).

C - Samples diffused with zinc, P-N junction formed, then mesa made.

TABLE VIII

Parameters Calculated from I-V Forward Characteristics for Various Treatments

Sample	I_o (amp)	n	Series Resistance at High forw'd currents (R_s)	Dot or Mesa Area (cm^2)	$R_s A$ (ohm cm^2)
A					
NA-1, AP62-2	1.2×10^{-12}	2.4	16.6 ohm	1.02×10^{-3}	16.9×10^{-3}
NA-4, bulk, poly	1.7×10^{-11}	4.4	11.4 "	6.68×10^{-4}	7.6×10^{-3}
NA-5, AP88-5	7×10^{-17}	2.2	5.4	7.35×10^{-4}	4.0×10^{-3}
B					
NA-4, bulk, poly	6.8×10^{-13}	2.5	7.5 ohm	5.90×10^{-4}	4.5×10^{-3}
NA-5, AP88-5	2.8×10^{-13}	2.6	10 "	6.78×10^{-4}	6.8×10^{-3}
C					
NA-1, AP62-2	8×10^{-10}	4	9.9 ohm	1.75×10^{-3}	17.3×10^{-3}
NA-4, bulk, poly	2.5×10^{-9}	3.6	6.0 "	2.6×10^{-3}	15.6×10^{-3}
NA-5, AP88-5	9.1×10^{-13}	3.1	6.1 "	3.0×10^{-3}	18.3×10^{-3}

A - Initial, starting material before diffusion or heat treatment.

B - Samples heat treated at 800° C (simulating diffusion schedule).

C - Samples diffused with zinc, P-N junction formed, then mesa made.

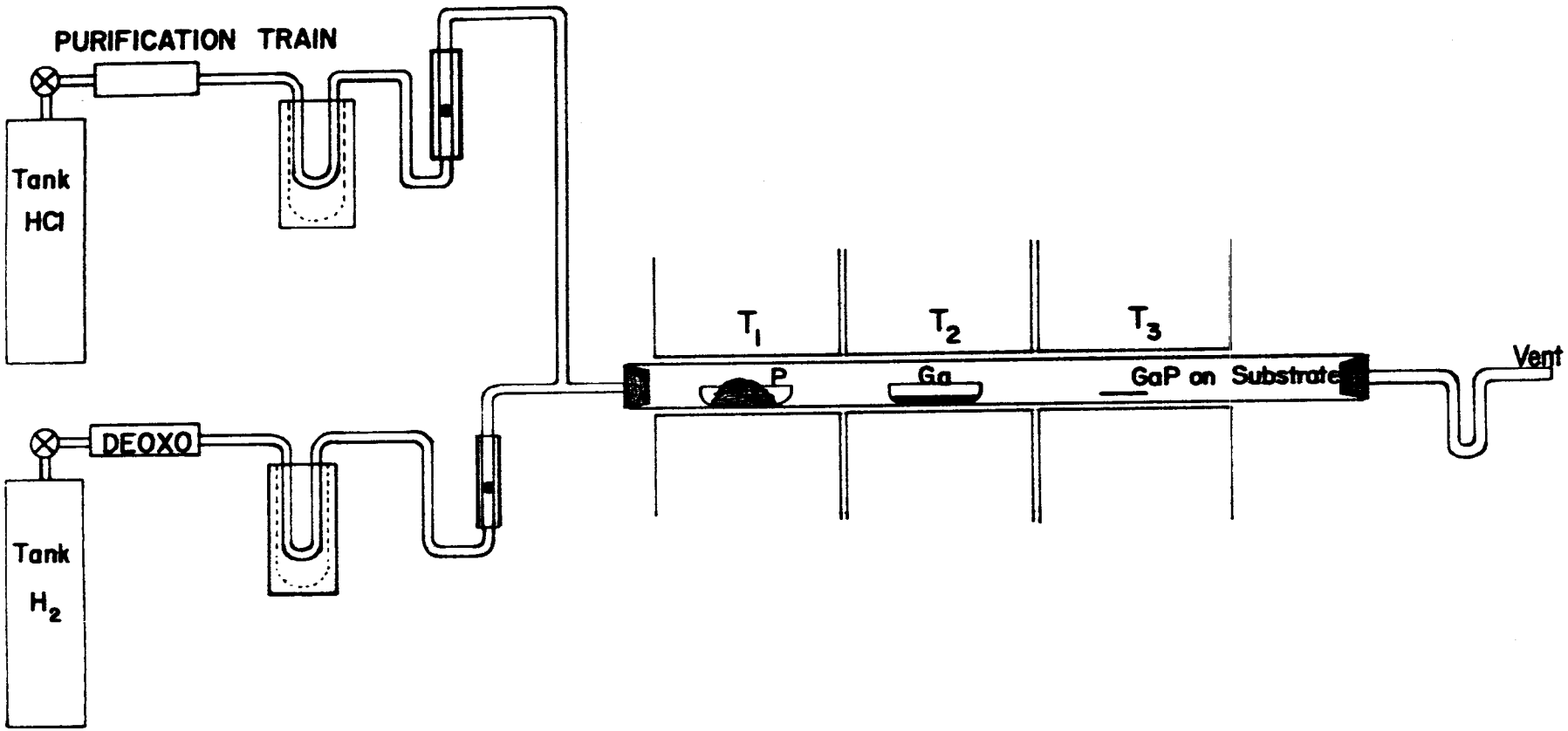

Figure 1

Schematic of system for growth of single crystal GaP by vapor phase deposition

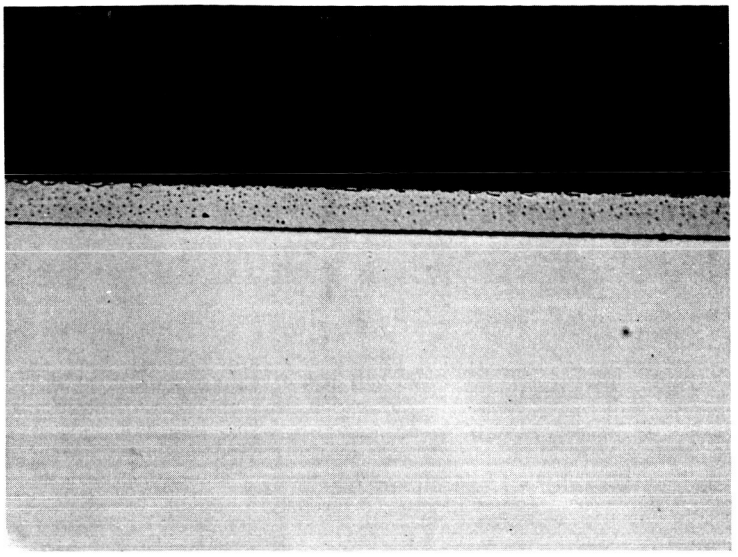

Figure 2

SC13-4 500x Cleaved and etched section showing smooth interface.

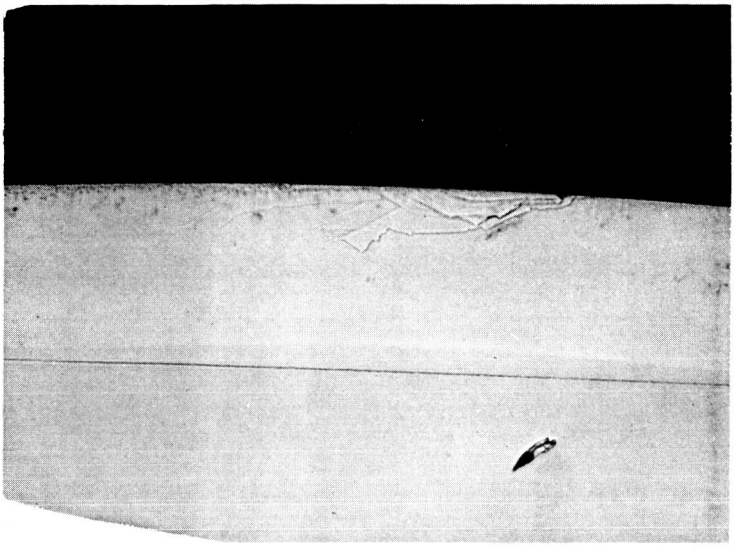

Figure 3

SC6-2 500x Very slightly ragged interface.

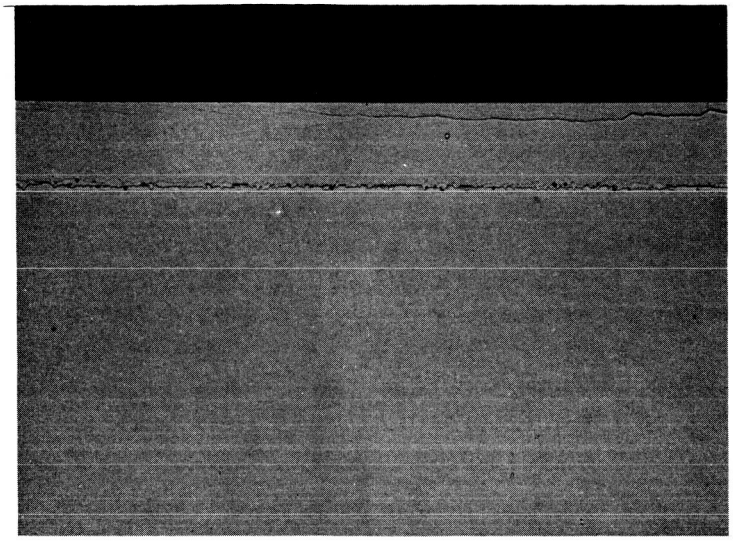

Figure 4

SC12-5 500x Slightly ragged interface.

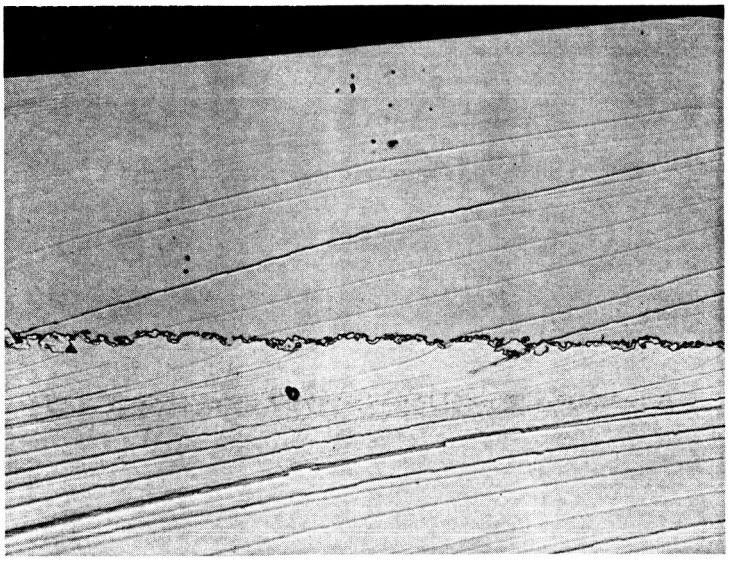

Figure 5

SC8-2 500x Ragged interface.

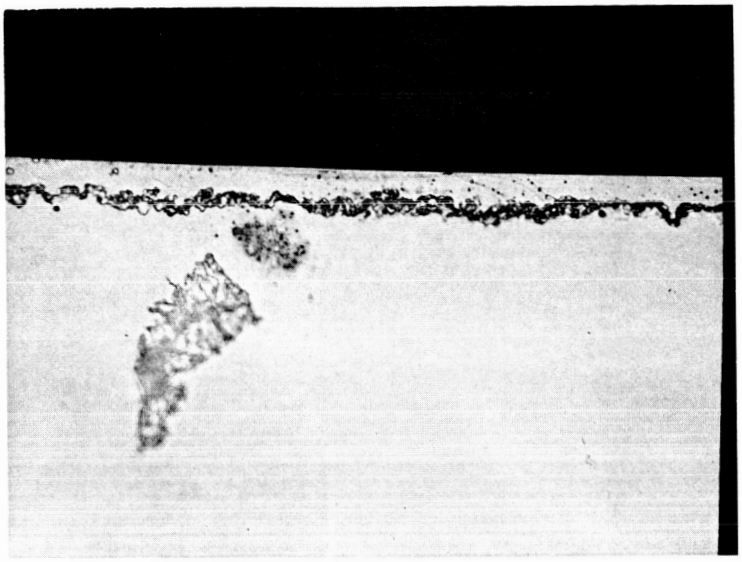

Figure 6

SC4-3 Very ragged interface.

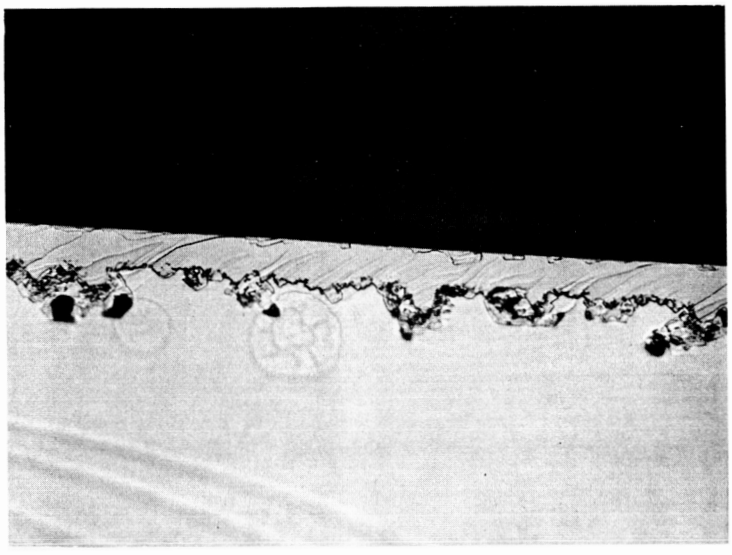

Figure 7

SC5-4 Extremely ragged interface with large voids.

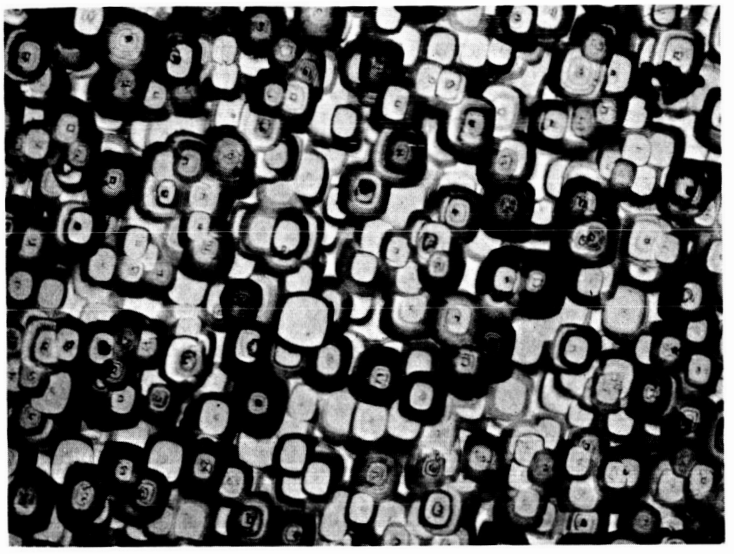

Figure 8

AP89-2 50x Typical bumps grown on <100> surface.

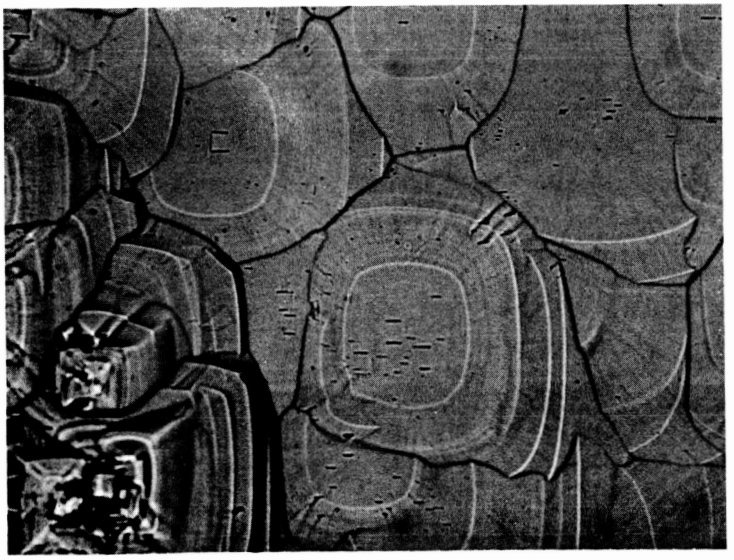

Figure 9

AP89-3 200x Typical bumps grown on <100> surface.

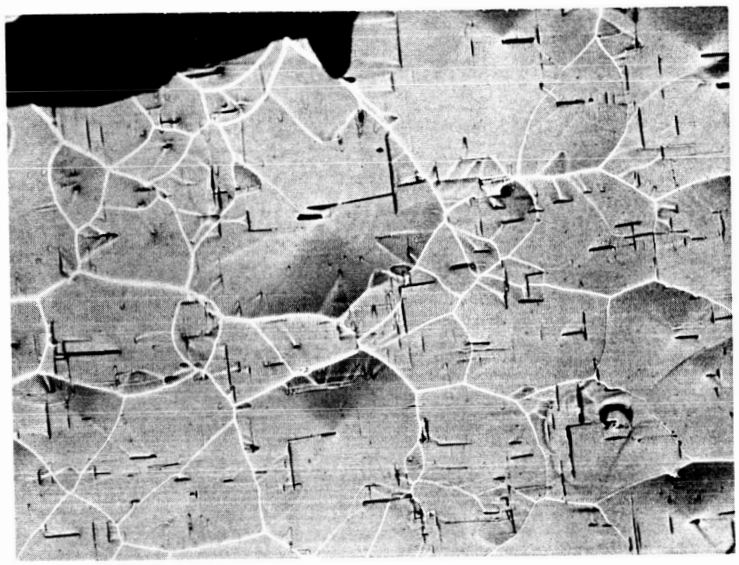

Figure 10

SC10-2 200x Epitaxial GaP surface covered with bumps and severe "hash marks". Apparent misorientation of the "hash marks" may be accounted for as intersections of <111> planes with slopes of the bumps.

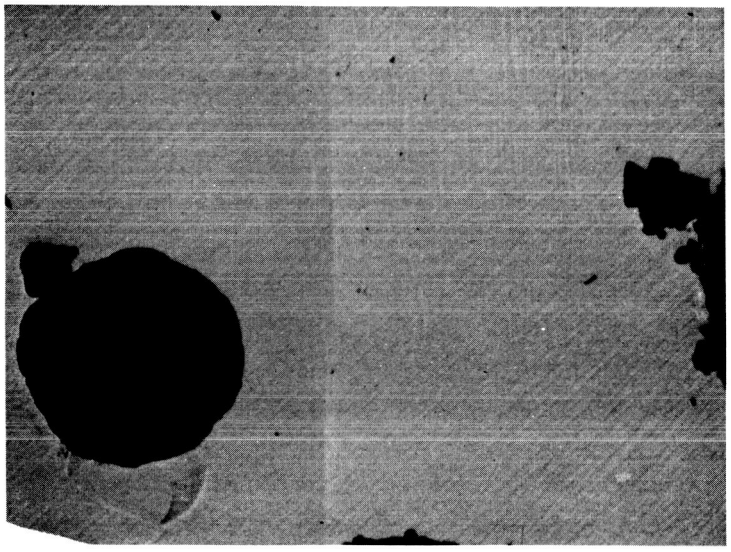

Figure 11

SC9-4 50x Smooth epitaxial GaP surface. Large dark spots are indium dots applied for electrical evaluation of the Hall bar. An incipient bump appears in the lower left corner partially hidden by an indium dot. The light vertical structures are surface scratches resulting from handling.

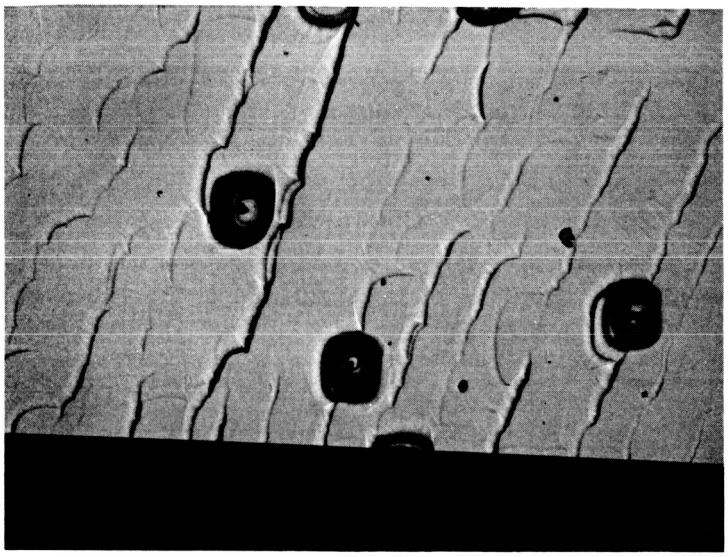

Figure 12

SC5-3 50x Top surface of epitaxial GaP layer near cleaved edge.

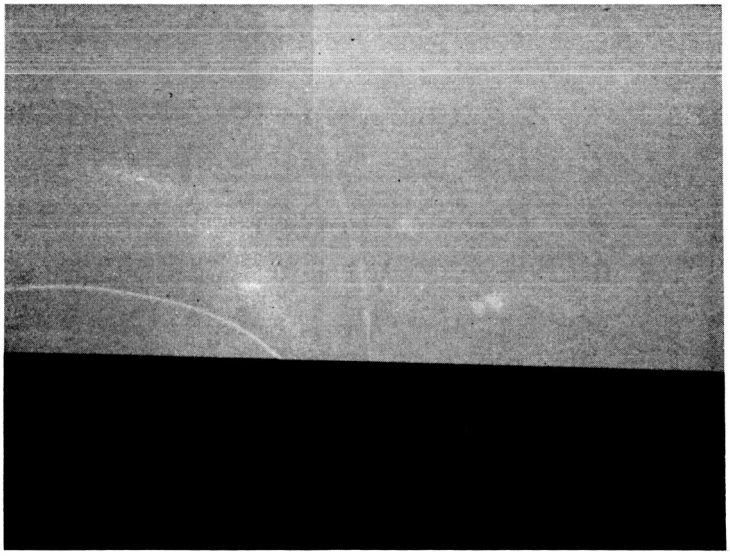

Figure 13

SC5-3 500x Same view as above enlarged. Faint light spots are voids (slightly out of focus) seen thru the transparent GaP layer. No "hash marks" evident even on slope of bump.

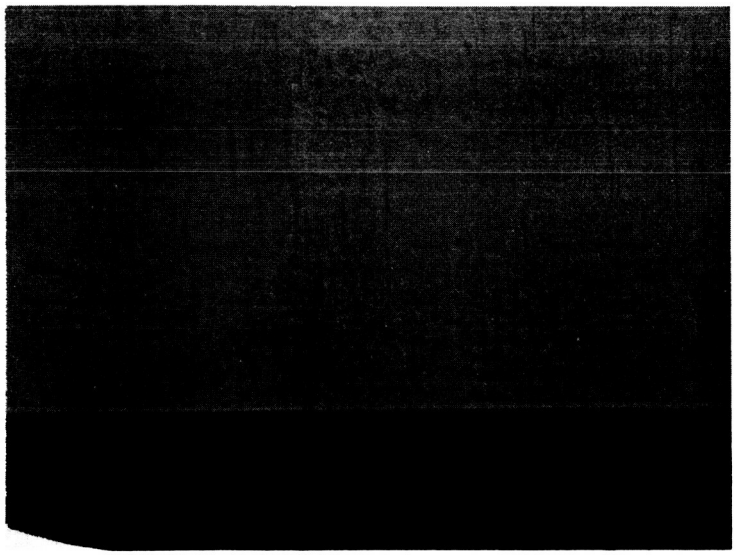

Figure 14

SC12-7 500x phase contrast. Top surface of epitaxial GaP layer near cleaved edge showing "hash marks", faint dark vertical lines perpendicular to edge.

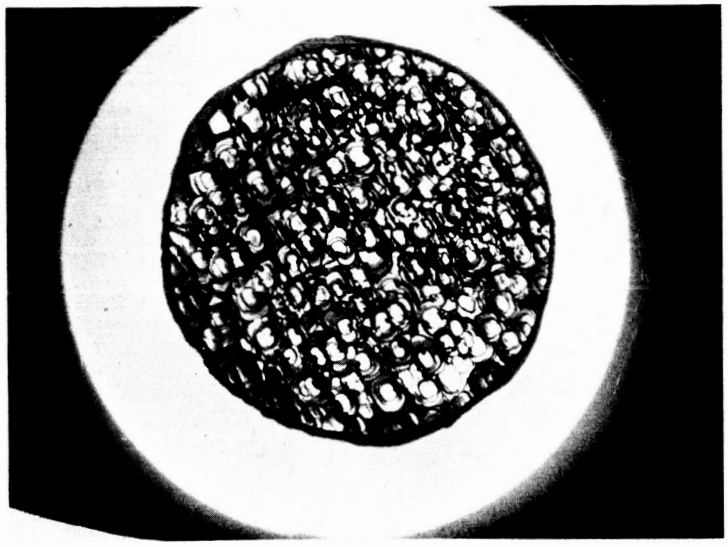

Figure 15

SC6/11 3.5x direct illumination from below, bottom side up, showing bump structure.

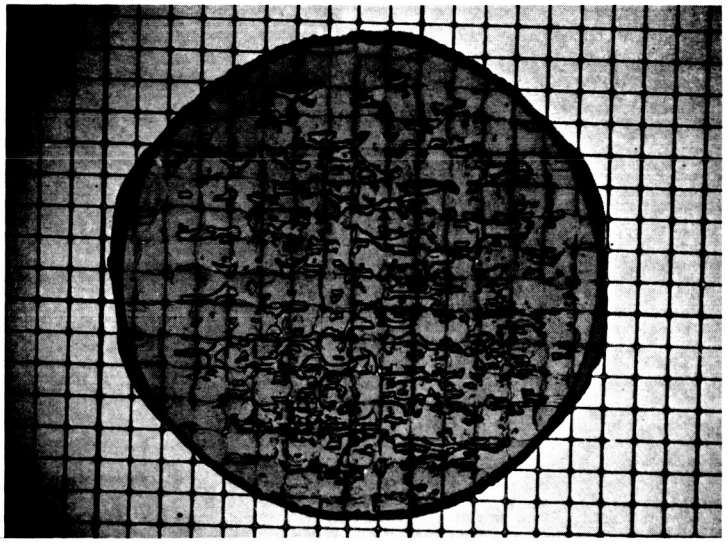

Figure 16

SC6/11 diffuse illumination from below, bottom side up, showing unfilled areas caused by cleaning deficiencies. Thickness at bottom of holes is a minimum of ~ 30μ. 1 mm. grid.

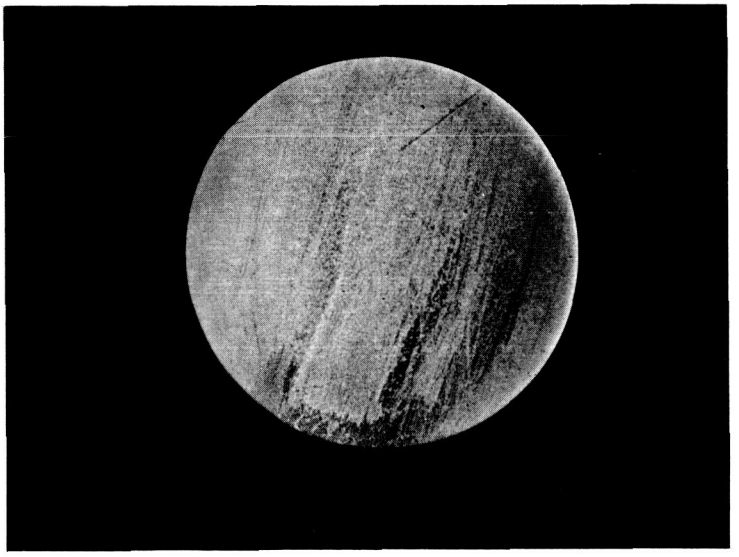

Figure 17

SC6/11 3.5x Bright field illumination of bottom. Etch figure exaggerated, but suggests association with distribution of residue remaining on cleaned GaAs substrate. Original interface very slightly ragged (see Figure 3). Rim of GaP extending beyond substrate roughened by lapping does not show.

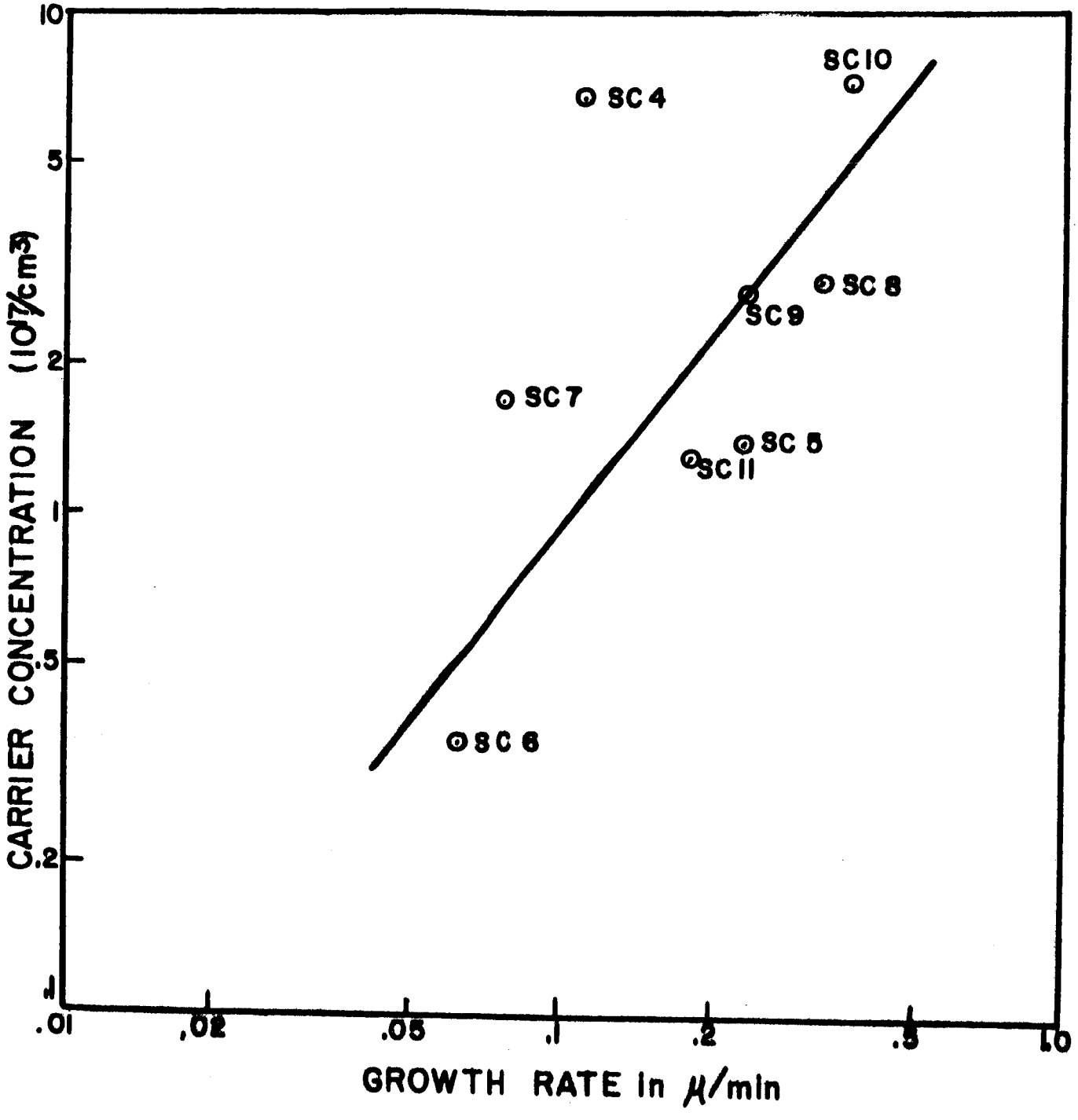

Figure 18

Carrier concentration vs. growth rate for series of depositions using gallium source with excess phosphorus.

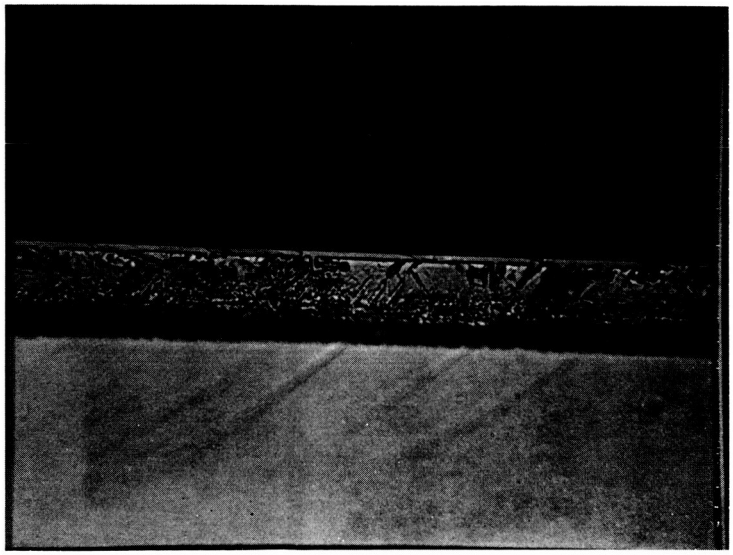

Figure 19

Sample NA-5, AP88-5 Sectioned to show P-N junction. Magnification - 500x; P layer depth - 2 μ, note ragged junction and relatively poor GaP-GaAs interface.

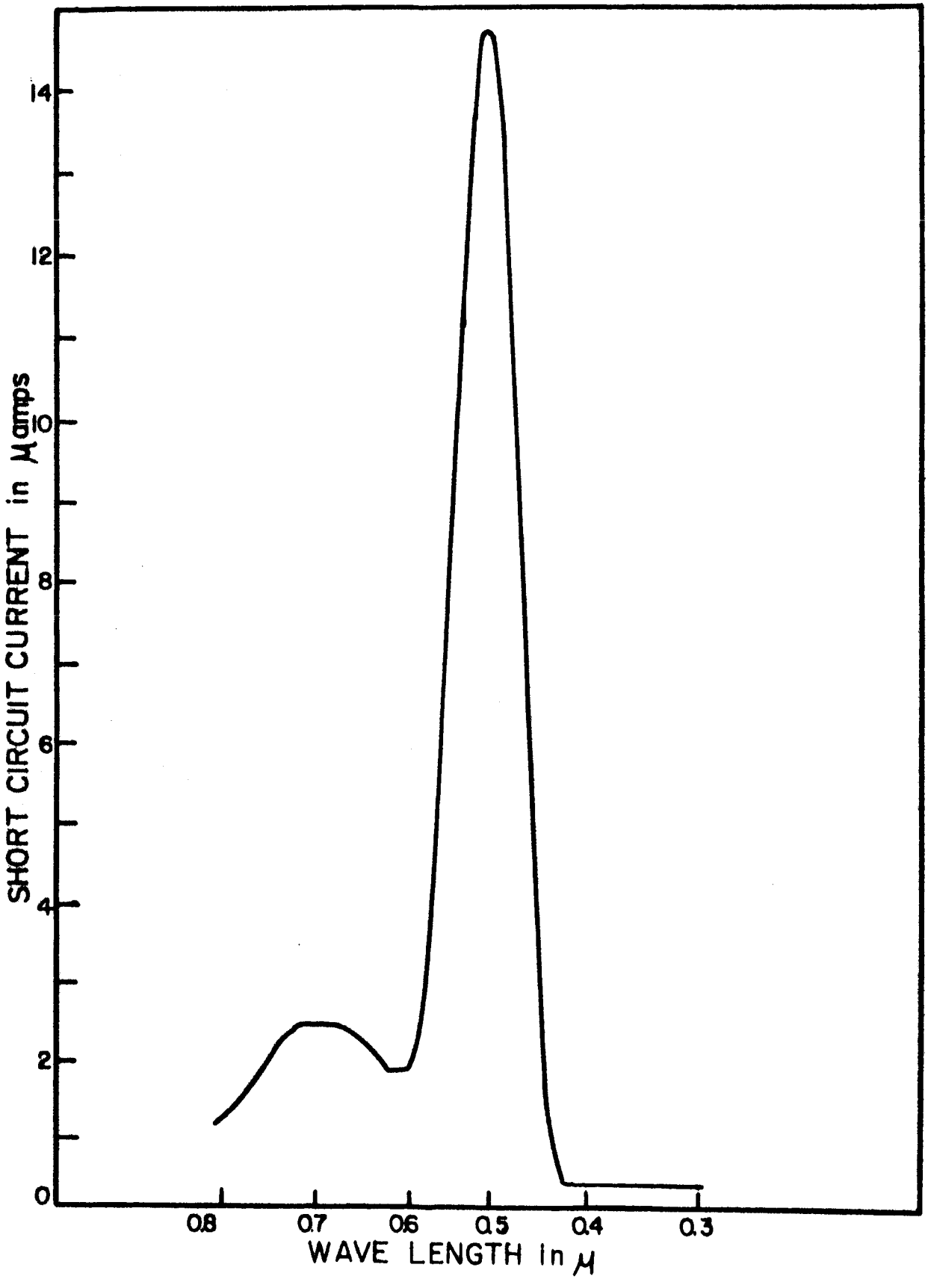

Figure 20 Typical spectral response curve as traced.

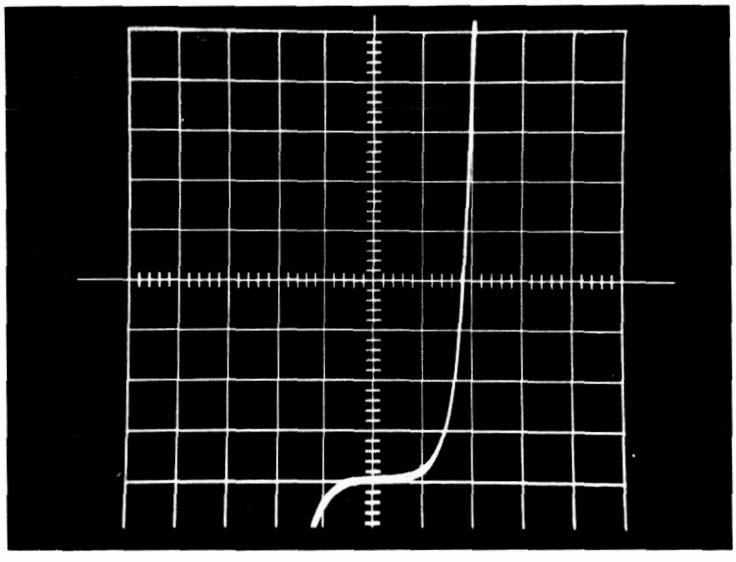

Figure 21

I-V trace of sample NA-5, AP88-5 current, vertical scale, .2 ma/cm, voltage, abscissa, .5 v/cm.

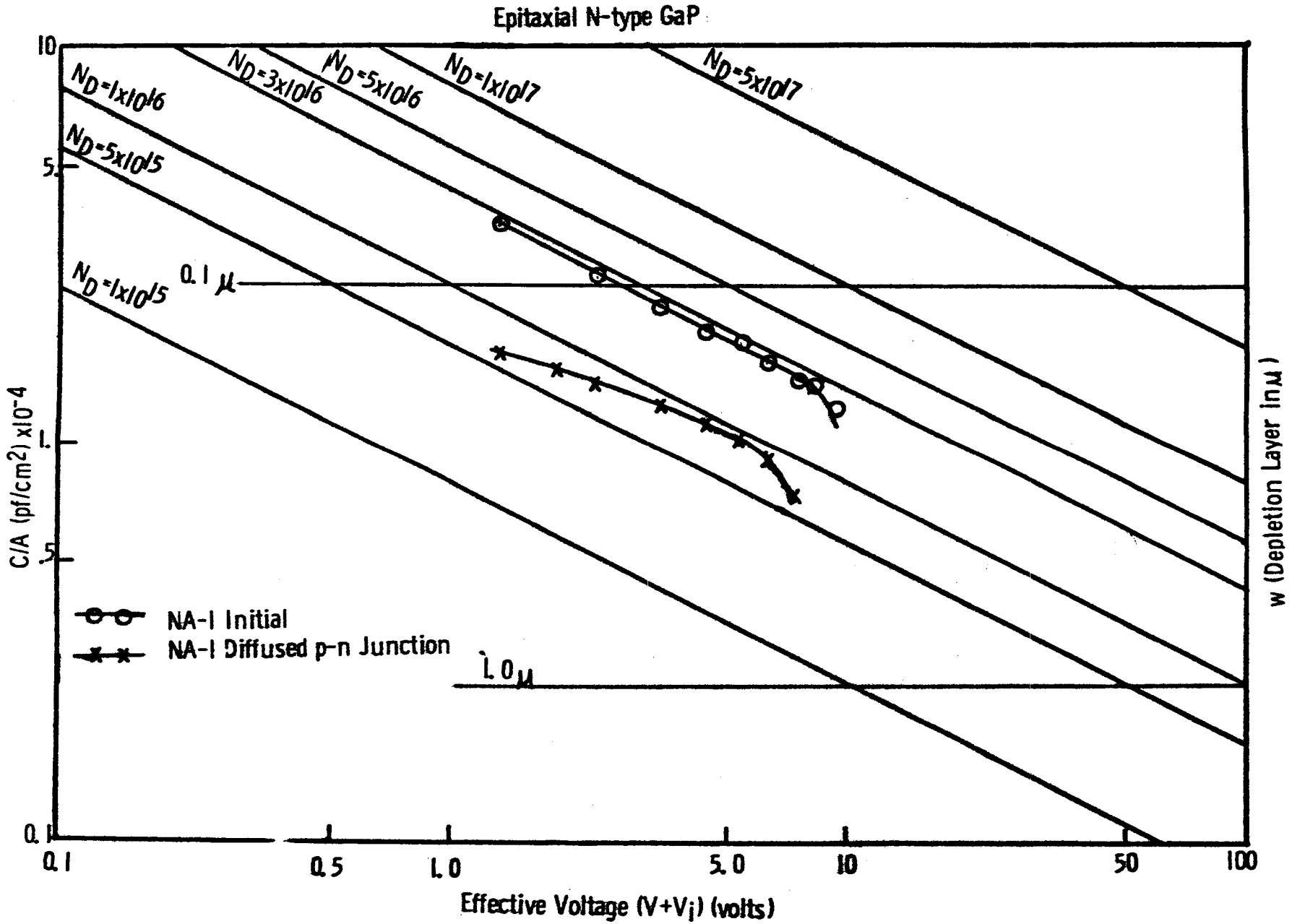

Figure 22

Capacity-voltage data of Sample NA-1 (see text).

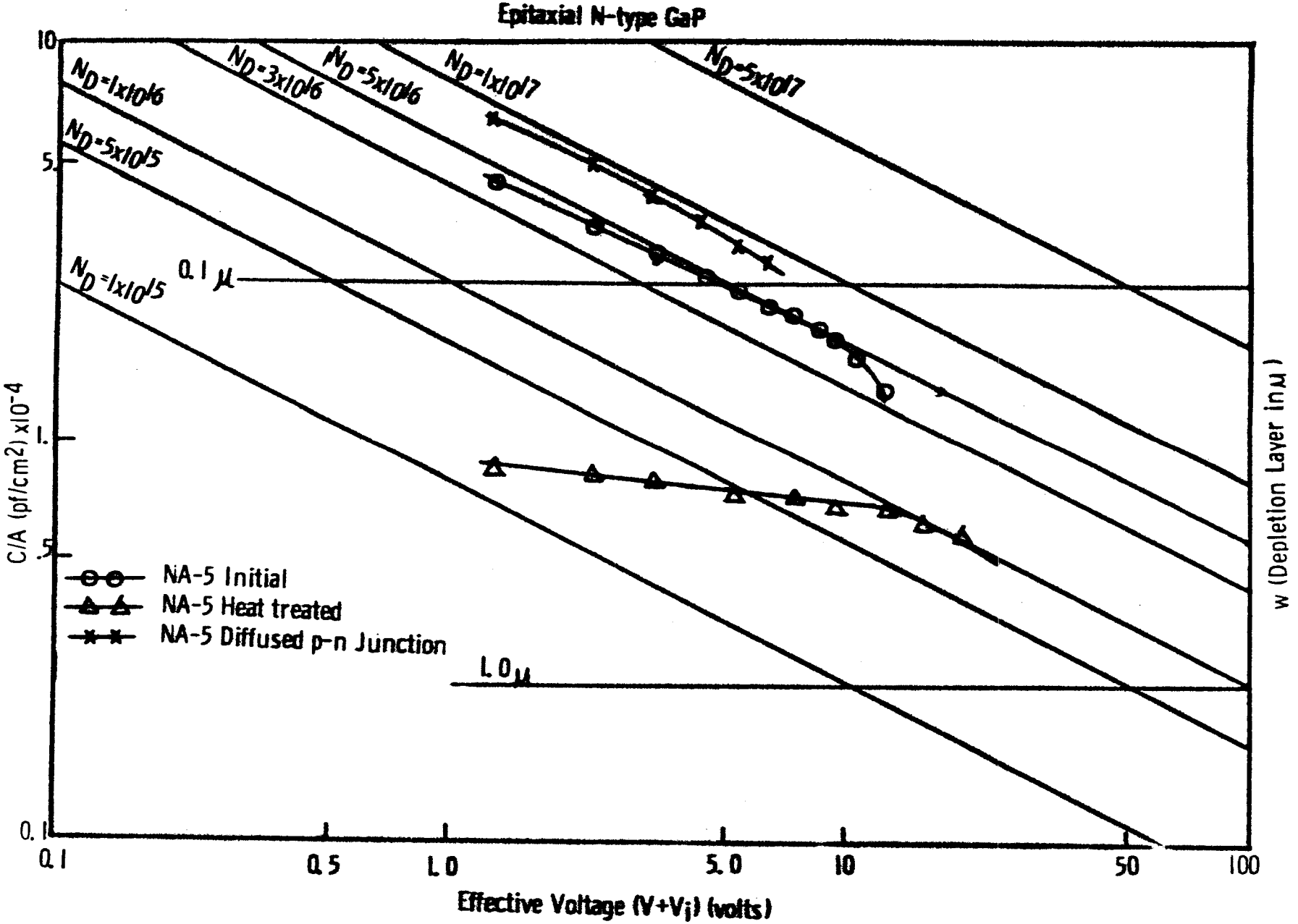

Figure 23

Capacity-voltage data of Sample NA-5 (see text).

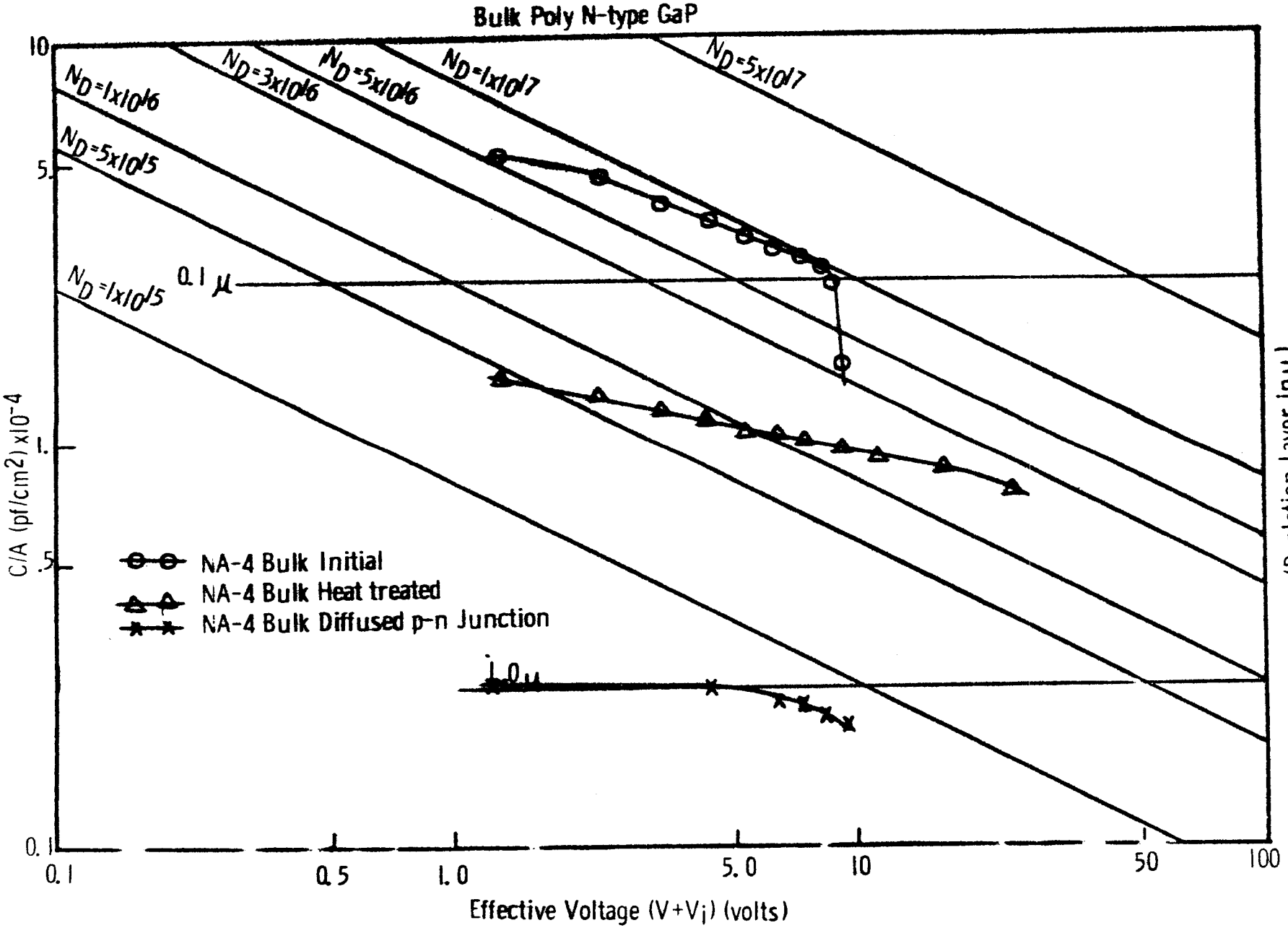

Figure 24

Capacity-voltage data of Sample NA-4 Bulk (see text).

DISTRIBUTION LIST

		No. of Copies
National Aeronautics and Space Administration Washington, D. C. 20546		
Attn:	Walter C. Scott/RP	1
	J. L. Sloop/RP	1
	Millie Ruda/AFSS-LD	1
National Aeronautics and Space Administration Scientific and Technical Information Facility Box 5700 Bethesda, Maryland 20546		3
National Aeronautics and Space Administration Goddard Space Flight Center Greenbelt, Maryland 20771		
Attn:	W. R. Cherry	1
	M. Schach	1
	B. Mermelstein, Code 672	1
	J. W. Callaghan, Code 621	1
	Librarian	1
National Aeronautics and Space Administration Lewis Research Center 21000 Brookpark Road Cleveland, Ohio 44135		
Attn:	J. J. Fackler, MS 86-1	1
	B. Lubarsky, MS 86-1	1
	H. Shumaker, MS 86-1	1
	R. L. Cummings, MS 86-1	1
	C. K. Swartz, MS 86-1	4
	N. D. Sanders, MS 302-1	1
	J. Broder, MS 302-1	1
	J. Mandelkorn, MS 302-1	1
	A. E. Potter, MS 302-1	1
	C. S. Corcoran, MS 100-1	1
	N. T. Musial, MS 77-1	1
	George Mandel, MS 5-5	1
National Aeronautics and Space Administration Langley Research Center Langley Station Hampton, Virginia 23365		
Attn:	W. C. Hulton	1
	E. Rind	1

DISTRIBUTION LIST

		No. of Copies
Wright Air Development Division Wright-Patterson Air Force Base Dayton, Ohio		
Attn:	P. R. Betheand	1
	Mrs. E. Tarrants/WWRNEM-1	1
Flight Accessories Aeronautics Systems Division Wright-Patterson AFB Dayton, Ohio		
Attn:	Joe Wise/ASRMFP-2	1
Aerospace Corporation P. O. Box 95085 Los Angeles 45, California		
Attn:	Dr. G. Hove	1
	Dr. F. Mozer	1
	V. J. Porfune	1
	Dr. I. Spiro	1
Battelle Memorial Institute 505 King Avenue Columbus, Ohio		
Attn:	L. W. Aukerman	1
	R. E. Bowman	1
	T. Shielladay	1
Bell and Howell Research Center 360 Sierre Madre Villa Pasadena, California		
Attn:	Alan G. Richards	1
Bell Telephone Laboratories Murray Hill, New Jersey		
Attn:	W. L. Brown	1
	U. B. Thomas	1
Clevite Research Center 540 E. 105th Street Cleveland, Ohio 44108		
Attn:	Dr. Hans Jaffe	1
The Eagle-Picher Company Chemical and Material Division Miami Research Laboratories 200 Ninth Avenue, N. E. Miami, Oklahoma		
Attn:	John R. Musgrave	1

DISTRIBUTION LIST

	No. of Copies
Jet Propulsion Laboratory 4800 Oak Grove Drive Pasadena, California 91103	
Attn: P. Goldsmith	1
G. E. Sweetnam	1
Institute for Defense Analysis Connecticut Avenue, N. W. Washington D. C. 20546	
Attn: R. Hamilton	1
Advanced Research Projects Agency Department of Defense, Pentagon Washington, D. C. 20546	
Attn: Dr. C. Yost	1
Naval Research Laboratory Department of the Navy Washington, D. C. 20546	
Attn: E. Broncato, Code 6464	1
M. Wotaw, Code 5170	1
Dr. V. Linnenbom, Code 7450	1
Dr. C. Klick, Code 6440	1
U. S. Army Advent Management Agency Mission Equipment Department Ft. Monmouth, New Jersey	
Attn: William Scherr, SIGFM/PAM-5	1
U. S. Army Signal Research and Development Laboratory Fort Monmouth, New Jersey	
Attn: Power Sources Branch	1
Air Force Cambridge Research Center Air Research and Development Command USAF, Hanscem Field Bedford, Massachusetts	
Attn: Col G. de Giacomo	1
Air Force Ballistic Missile Division Air Force Unit Post Office Los Angeles 45, California	
Attn: COL L. Norman, SSEM	1
LT COL G. Austin, SSZAS	1
CAPT A. Johnson, SSZDT	1
CAPT W. Hoover, SSTRE	1
LT COL A. Bush, SSZME	1

DISTRIBUTION LIST

	No. of Copies
Harshaw Chemical Company Solid-State Division 2240 Prospect Avenue Cleveland, Ohio 44115 Attn: James C. Schaefer	1
Heliotek Corporation 12500 Gladstone Avenue Sylmar, California Attn: Eugene Ralph	1
Hughes Aircraft Company Aerospace Group, R and D Division Culver City, California Attn: C.A. Escoffery	1
Leesona Moos Laboratories 90-28 Van Wyck Expressway Jamaica 18, New York Attn: Stanley Wallack	1
National Cash Register Company Physical Research Department Dayton 9, Ohio Attn: R. R. Chamberlin	1
North American Aviation, Inc. Autonetics Division Anaheim, California Attn: R. R. August	1
Philco Corporation Blue Bell, Pennsylvania Attn: Mr. A. E. Mace	1
Radio Corporation of America RCA Re search Laboratories Princeton, New Jersey Attn: P. Rappaport	1
Radio Corporation of America Semiconductor and Materials Division Somerville, New Jersey Attn: Dr. F. L. Vogel	1
Sandia Corporation Albuquerque, New Mexico Attn: F. Smits	1

DISTRIBUTION LIST

	No. of Copies
Solid-State Electronics Laboratory Stanford Electronics Laboratories Stanford University Stanford, California Attn: Prof. G. L. Pearson	1
Westinghouse Electric Corporation Research and Development Laboratories Churchill Borough, Pennsylvania Attn: H. C. Chang	1
Westinghouse Electric Corporation Semiconductor Division Youngwood, Pennsylvania Attn: Don Gunther	1